

Review

## Energy Storage in Bifunctional TiO<sub>2</sub> Composite Materials under UV and Visible Light

Liangbin Xiong<sup>1,2</sup>, Jialin Li<sup>1</sup> and Ying Yu<sup>1,\*</sup>

<sup>1</sup> Institute of Nanoscience and Nanotechnology, Huazhong Normal University, Wuhan 430079, China; E-Mail: lijil@phy.ccnu.edu.cn

<sup>2</sup> Physics Department, Huanggang Normal University, Huanggang, 438000, China; E-Mail: xionglb2004@yahoo.com.cn

\* Author to whom correspondence should be addressed; E-Mail: yuying@phy.ccnu.edu.cn; Tel.: +86-27-67867037; Fax: +86-27-67861185.

Received: 30 September 2009 / Accepted: 28 October 2009 / Published: 6 November 2009

---

**Abstract:** This paper provides an overview of recent studies on energy storage in bifunctional TiO<sub>2</sub> composite materials under UV and visible light. The working mechanism, property improvements and applications of these bifunctional TiO<sub>2</sub> composite systems are introduced, respectively. The latest results obtained in our laboratory, especially a new process for photoelectric conversion and energy storage in TiO<sub>2</sub>/Cu<sub>2</sub>O bilayer films under visible light, are also presented. Hopefully this review will stimulate more fundamental and applied research on this subject in the future.

**Keywords:** photoelectric conversion; energy storage; TiO<sub>2</sub>; Cu<sub>2</sub>O; WO<sub>3</sub>; Ni(OH)<sub>2</sub>

---

### 1. Introduction

The economic growth in many parts of the World during the past decade was sustainable thanks to affordable energy prices. The dependence on oil and electricity has made energy an important component in our everyday life and the recent increases of oil and gas prices have prompted everyone to take a careful look at energy issue. In the 20th century, the population has quadrupled and our energy demand went up 16 times. The exponential energy demand is exhausting our fossil fuel supply at an alarming rate [1,2]. About 13 terawatts (TW) of energy is currently needed to sustain the lifestyle of 6.5 billion people worldwide. By 2050, it is estimated we will need an additional 10 TW of clean

energy to maintain the current lifestyle. In order to meet the increasing energy demands in the near future, we will be forced to seek environmentally clean alternative energy resources [3,4]. Three major options are at our disposal to tackle the generation of 10 TW of clean energy in the coming years. These include carbon neutral energy (fossil fuel in conjunction with carbon sequestration), nuclear power, and various forms of renewable energy. Among these last options, solar energy stands out as the most viable choice to meet the energy demand. Despite the vast size of this resource, the energy produced from solar sources remains less than 0.01% of the total energy demand [5].

Nearly all energy consumed in our planet comes from the solar light, either in a roundabout way or directly in the form of heat and light radiation. The effective utilization of clean, safe, abundant and regenerated solar energy will lead to promising solutions. not only for energy issues due to the exhaustion of nature energy sources. but also for many problems caused by environmental pollution. Sunlight can be converted into other forms of energy by a variety of methods. Generally speaking, the first step to utilize solar light is conversion, by which we can use it in our own way. The second is storage, by which we can store excess energy in the day time and use it during the night or any other time when the visible light available is insufficient.

Photoelectric conversion is one of the most widely-used and well-developed techniques in the field of solar energy utilization today. The photovoltaic (PV) industry is booming, with an estimated growth rate in excess of 30% per year over the last decade [6]. Crystalline silicon solar cells, which are presently demonstrated to have energy conversion efficiencies close to 25%, account for the most important part of the world PV market [7,8]. Dye sensitized solar cells, which have already reached conversion efficiencies exceeding 11%, offer the prospect of the low cost fabrication without expensive and energy-intensive high temperature and high vacuum processes to facilitate market entry [9]. Thin film PV technologies based on inorganic materials are developing rapidly both in the laboratory and in industry [6]. They are also a formidable competitor aiming to boost their market share.

However, these traditional photovoltaic materials generally function as photoelectric or chemical energy conversion devices under irradiation. The excess energy produced by these devices has to be stored by energy storage systems such as electrochemical storage cells or supercapacitors [10]. The existence of the energy storage systems always results in an increase of expense and the consumption of extra energy. Now that traditional photovoltaic materials cannot play the role of energy storage and traditional energy storage systems do not have the ability of photoelectric conversion, their combination should be a new promising field in the development and utilization of solar energy.

TiO<sub>2</sub> nanostructure hybrid materials are the focus of both fundamental and applied research [11]. Nanohybrid materials developed by the modification of pristine TiO<sub>2</sub> with anions, cations, and metals are named second-generation TiO<sub>2</sub> photocatalysts [12]. Electron transfer between a TiO<sub>2</sub> substrate and the interfused material endows them with novel properties, such as absorption of visible light and enhanced light electricity conversion efficiency and improved activity in photocatalysis [13-15], which can be used in quantum dot solar cells [16,17] and gas sensors [18]. In recent years, functionalized TiO<sub>2</sub> hybrid materials were also reported as energy storage materials.

In 2000, Zou's group found that TiO<sub>2</sub>/carbon fiber electrodes prepared by laser deposition had dual functions of opto-electric conversion and electrochemical energy storage. Since 2001, a few Japanese research groups have developed several TiO<sub>2</sub> composite systems with dual abilities of photoelectric

conversion and energy storage (bifunctional composite system) and a few similar TiO<sub>2</sub> composite systems were developed in recent years by other groups. This is a very new research field that has not yet been paid the deserved attention. Incidentally, the application for TiO<sub>2</sub> composite system in solar energy has been overviewed extensively [9,19,20], but that for both photoelectric conversion and energy storage of solar energy has not yet been reviewed until now. So, according to the publications and the research carried out in our laboratory, a general overview of the subject of energy storage in TiO<sub>2</sub> composite systems under solar light is presented here.

## 2. Survey of Bifunctional TiO<sub>2</sub> Composite Materials

In 2000, TiO<sub>2</sub> composite materials with energy storage abilities were first developed by Xinjing Zou's group [21] who found that TiO<sub>2</sub>/carbon fiber electrodes functioned as a photo-rechargeable battery with the dual functions of opto-electric conversion and electrochemical energy storage. In 2001, Tatsuma *et al.* [22] developed a TiO<sub>2</sub>/WO<sub>3</sub> photoelectrochemical anticorrosion system with energy storage ability. A TiO<sub>2</sub> coating is coupled with a WO<sub>3</sub> coating as an electron pool, in which the reductive energy can be stored. Since then, TiO<sub>2</sub>/MoO<sub>3</sub> [23], SrTiO<sub>3</sub>/WO<sub>3</sub> [24], TiO<sub>2</sub>/phosphotungstic acid (PWA) [25], TiO<sub>2</sub>/Ni(OH)<sub>2</sub> [26] and several other TiO<sub>2</sub>/WO<sub>3</sub> [27-29] composite systems have also been developed by the groups of Tetsu Tatsuma and his collaborators. The energy can be stored either in reduced WO<sub>3</sub>, MoO<sub>3</sub>, PWA or in oxidized Ni(OH)<sub>2</sub> under UV light. In 2003, Raghavan *et al.* [30] showed that SnO<sub>2</sub> coupled with TiO<sub>2</sub> can store reductive energy generated on UV illumination of TiO<sub>2</sub>, which enables the continued cathodic protection effect under dark conditions. In 2008, Yasomanee *et al.* [31] reported that TiO<sub>2</sub>/Cu<sub>2</sub>O composite films showed a multi-electron storage ability under UV-vis irradiation. It was noticed that the irradiation of ITO/TiO<sub>2</sub>/Cu<sub>2</sub>O led to the formation of trapped electrons and this stored energy resulted in H<sub>2</sub> evolution from H<sub>2</sub>O, even in the dark. Additionally, Chien-Tsung Wang [32] demonstrated that V<sub>2</sub>O<sub>5</sub> served as an energy storage material to accumulate photoelectrons generated by the TiO<sub>2</sub> semiconductor, due to the relative energy levels of the conduction bands of V<sub>2</sub>O<sub>5</sub> and TiO<sub>2</sub>. In 2009, Zhang's [33], Zhao's [34] and Tatsuma's [35] groups reported that optical energy can be stored by TiO<sub>2</sub> nanotube array/Ni(OH)<sub>2</sub> composite electrodes, WO<sub>3</sub>/TiO<sub>2</sub> nanohybrid materials and Au-TiO<sub>2</sub>/WO<sub>3</sub> systems, respectively. It is worth mentioning that the Au-TiO<sub>2</sub> composite system, which is based on plasmon resonance absorption of Au nanoparticles, can store reductive energy in WO<sub>3</sub> under visible-light irradiation. Recently, our group found that visible-light energy can be stored by Ti<sup>3+</sup> in TiO<sub>2</sub>/Cu<sub>2</sub>O bilayer film [36]. The appearance of visible-light induced energy storage system is a significant progress in this field and beneficial practical application since it can work directly under solar light.

## 3. Working Mechanism of Optical Energy Storage

The energy can be stored by reduced materials (such as WO<sub>3</sub>, MoO<sub>3</sub> and PWA), oxidized ones (Ni(OH)<sub>2</sub>) or TiO<sub>2</sub> itself. Zou's group described the double functions of opto-electric conversion and electrochemical energy storage for TiO<sub>2</sub>/carbon fiber electrodes by the characterization of photo charge and discharge currents. The systematic research on the mechanism of optical energy storage was first done by Tatsuma's group. Based on their and our own work, we here introduce three representative optical energy storage mechanisms.

### 3.1. Reductive Energy Storage in $\text{TiO}_2/\text{WO}_3$ ( $\text{MoO}_3$ or PWA) Composite System

Figure 1 shows the mechanism of reductive energy storage by  $\text{TiO}_2/\text{WO}_3$  composite system [27]. In this system, an excited electron and a corresponding hole are generated on  $\text{TiO}_2$  under UV light:



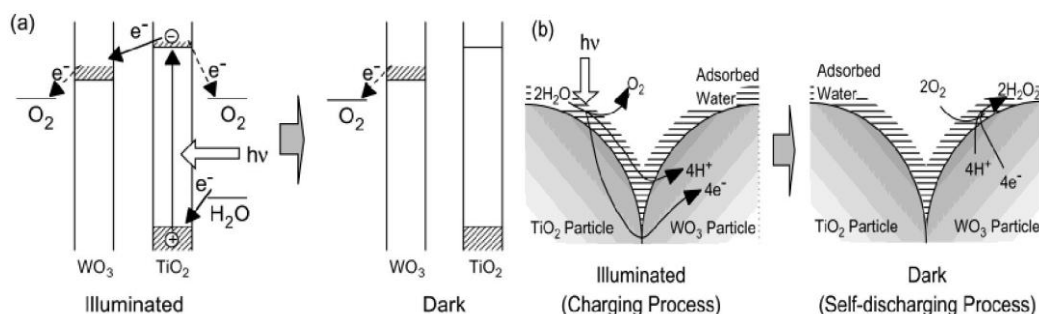
The electron may be transported through  $\text{TiO}_2$  (n-type semiconductor) to  $\text{WO}_3$ , and if so, a cation should be intercalated into  $\text{WO}_3$ . In pure water, only  $\text{H}^+$  is available as a cation:



On the other hand, the hole should also be consumed at the  $\text{TiO}_2$  surface by  $\text{H}_2\text{O}$  to generate chiefly  $\text{O}_2$  and  $\text{H}^+$ . Thus,  $\text{H}^+$  is generated by  $\text{TiO}_2$  (Equation 3) and is consumed by  $\text{WO}_3$  (Equation 2):



**Figure 1.** (a) Mechanism of reductive energy storage of  $\text{TiO}_2/\text{WO}_3$  composite system [28]. (b) Proposed models of electron and ion transfer in the charging and self-discharging processes of the  $\text{TiO}_2/\text{WO}_3$  composite film in humid air [27].

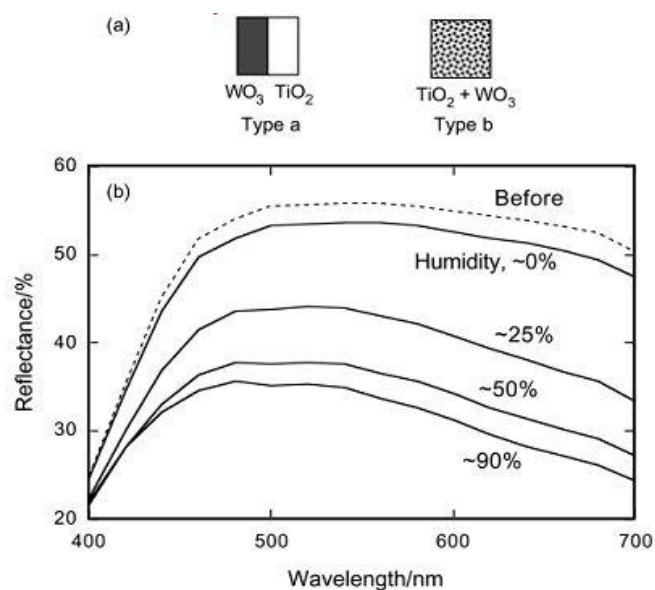


The ITO electrode coated with the  $\text{TiO}_2/\text{WO}_3$  composite film (type b, thick film, Figure 2a) was subjected to the 1 h UV irradiation in air to show the formation of  $\text{H}_x\text{WO}_3$ . As shown in Figure 2b, the behavior strongly depended on the relative humidity of the atmosphere. The film was well-colored in a humid atmosphere (relative humidity  $\geq 25\%$ ), while it was not colored well in a dry atmosphere. The color of  $\text{H}_x\text{WO}_3$  is blue. The reduction of  $\text{WO}_3$  (almost colorless) gave rise to the decrease in the reflectance shown in Figure 2b.

This can be explained in terms of ionic conductivity of the film surface. In the humid atmosphere, an adsorbed water layer should form on the film surface. This layer and the surface hydroxyl groups, of which dissociation should be facilitated by this water layer, should contribute to the ionic conduction. It is necessary for the photoelectrochemical reduction of  $\text{WO}_3$  (Figure 1b). To the contrary, in the dry atmosphere, the adsorbed water layer is almost absent so that the ionic conductivity should not be sufficient for the  $\text{WO}_3$  reduction.

As the excess electrons are accepted by  $\text{WO}_3$  and more  $\text{H}_x\text{WO}_3$  is generated, the reductive energy can be stored by  $\text{WO}_3$  in pure water, humid air or solution. It can be seen that  $\text{WO}_3$  retains the reductive energy for a certain period even after the light is turned off (Figure 1a).

**Figure 2.** (a) Schematic models for  $\text{TiO}_2/\text{WO}_3$  separated films (type a) and  $\text{TiO}_2/\text{WO}_3$  composite film (type b). (b) Changes in the reflectance of the  $\text{TiO}_2/\text{WO}_3$  composite film (type b, thick film) after UV irradiation ( $22 \text{ mW cm}^{-2}$ , 20 min) at a relative humidity of about 0, 25, 50, and 90% [27]. Reproduced with permission from the ACS, ©2002.

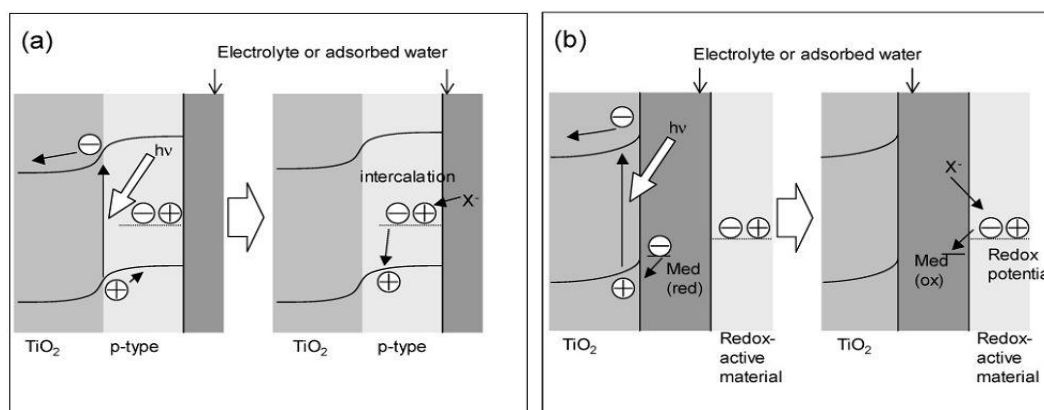


### 3.2. Oxidized Energy Storage in $\text{TiO}_2/\text{Ni}(\text{OH})_2$ Composite System

Two kinds of models for storing the oxidative energy of  $\text{TiO}_2$  were proposed, the p-n junction model and the mediation model (Figure 3) [26]. In the former, a redox-active p-type semiconductor is combined with  $\text{TiO}_2$  to form a p-n junction (Figure 3a).

Holes generated at the junction are separated from excited electrons and transported into the bulk of the p-type semiconductor for the oxidative energy storage. The electrical neutrality will be retained by the intercalation of the anions or the deintercalation of the cations so that oxidative energy will keep stable. In the mediation model (Figure 3b), an oxidant like  $\text{O}_2$ , which is photocatalytically produced by the oxidation of water adsorbed on  $\text{TiO}_2$ , diffuses and oxidizes a redox-active material.

**Figure 3.** Models for the oxidative energy storage photocatalysts. (a) p-n junction model and (b) mediation model [26].



Ni(OH)<sub>2</sub> is reported to be a p-type semiconductor [37,38], and is known as a cathode active material of secondary batteries [39] with relatively positive redox potential (+0.5 to +0.6 V vs Ag|AgCl). Therefore, it is expected to be suitable for oxidative energy storage. After a TiO<sub>2</sub>/Ni(OH)<sub>2</sub> bilayer film was irradiated with UV light (365 nm; 10 mW cm<sup>-2</sup>) in pH 10 buffer, the film turned to brown as did the electrochemically oxidized film. Actually, the visible absorption spectrum of the irradiated film looked like that of the electrochemically oxidized film. These results suggest that the irradiation gave rise to the oxidation of Ni(OH)<sub>2</sub>. However, a Ni(OH)<sub>2</sub> film without TiO<sub>2</sub> was not colored under UV-irradiation. Therefore, TiO<sub>2</sub> should contribute to the photooxidation of Ni(OH)<sub>2</sub>. The brown-colored film could be turned back to colorless by electrochemical reduction. Namely, the photoelectrochemically stored oxidative energy could be taken out and used.

The photooxidation of Ni(OH)<sub>2</sub> most probably proceeds as follows. Electrons are photoexcited from the valence band to the conduction band (e<sup>-</sup><sub>CB</sub>) in TiO<sub>2</sub> or at the TiO<sub>2</sub>/Ni(OH)<sub>2</sub> junction (Equation 1). The correspondingly formed holes in the valence band (h<sup>+</sup><sub>VB</sub>) accept electrons from Ni(OH)<sub>2</sub>, either directly or indirectly (Equation 4):



The photo-excited electrons should be consumed by an electron acceptor, most likely dissolved oxygen diffused to the TiO<sub>2</sub> surface through the pores in the Ni(OH)<sub>2</sub> layer because of a reaction such as Equations 5a or 5b:



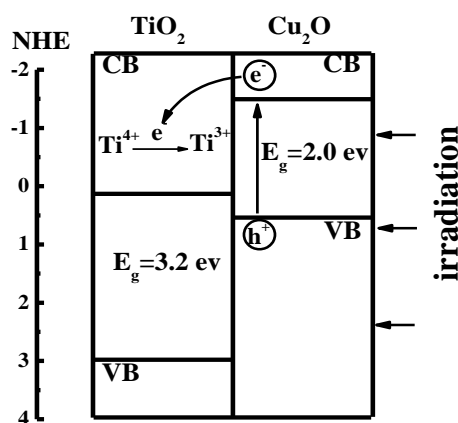
At the current stage, it is uncertain whether the oxidative energy storage is based on the p-n junction model (Figure 1a) or the mediation model (Figure 1b). According to the literature [40], TiO<sub>2</sub> is known to form a p-n junction with NiO. Ni(OH)<sub>2</sub> is also reported to be a p-type semiconductor similar to NiO [30]. Hence, it is possible that a p-n junction forms at the TiO<sub>2</sub>/Ni(OH)<sub>2</sub> interface. If the mediation model worked, the mediator might be, for example, the H<sub>2</sub>O<sub>2</sub> generated by Equation 5b. However, a Ni(OH)<sub>2</sub> film without TiO<sub>2</sub> was not oxidized when it was exposed to 0.1–10 M H<sub>2</sub>O<sub>2</sub> with or without UV light. Rather, oxidized Ni(OH)<sub>2</sub> was reduced by H<sub>2</sub>O<sub>2</sub> in the dark. Thus, the mediator, if any, is more likely to be an oxidant other than H<sub>2</sub>O<sub>2</sub>. If the energy storage proceeded according to the p-n junction model, the efficiency would be improved by increasing the junction area, for instance, by making the TiO<sub>2</sub> layer porous. On the other hand, if the mediation model worked, the distance between Ni(OH)<sub>2</sub> and TiO<sub>2</sub> could be optimized so as to suppress the rereduction by the electrons on TiO<sub>2</sub>.

In all, although it is uncertain whether the oxidative energy storage is based on the p-n junction model or the mediation model, it is sure that the energy stored in Ni(OH)<sub>2</sub> is oxidized energy, which is different from that in WO<sub>3</sub> according to their color changes and results of photoelectrochemical experiments.

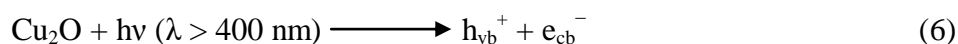
### 3.3. Multi-electrons Energy Storage in TiO<sub>2</sub>/Cu<sub>2</sub>O Composite System

Recently, we prepared a TiO<sub>2</sub>/Cu<sub>2</sub>O bilayer film on doped fluorine SnO<sub>2</sub> (FTO) conducting glass according to literature [41,42]. Ti<sup>3+</sup> in the TiO<sub>2</sub>/Cu<sub>2</sub>O bilayer film is demonstrated to store energy under visible light. It is well known that the band gap of TiO<sub>2</sub> is about 3.2 eV and the conduction band of TiO<sub>2</sub> is about -0.2 eV [43]. Cu<sub>2</sub>O is a semiconductor with one of the highest conduction bands. The band gap of Cu<sub>2</sub>O is about 2.0 eV and the potential of its conduction band is -1.4 eV [44].

**Figure 4.** Sketch of interfacial electron transfer in TiO<sub>2</sub>/Cu<sub>2</sub>O bilayer film [36].

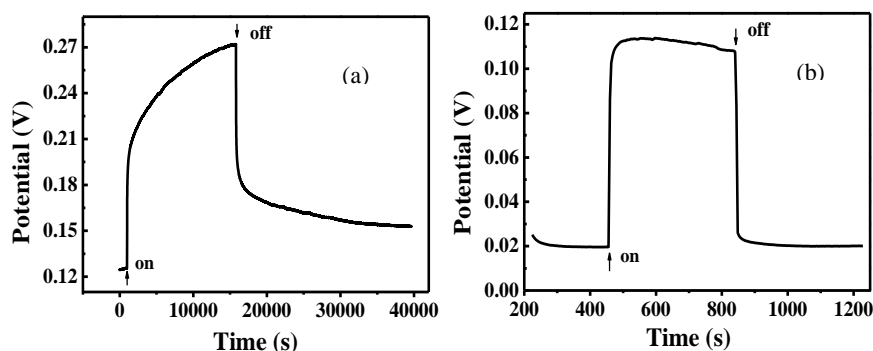


As shown in Figure 4, the photogenerated electrons from the conduction band of Cu<sub>2</sub>O were captured by Ti<sup>4+</sup> ions in TiO<sub>2</sub> and Ti<sup>4+</sup> ions were further reduced to Ti<sup>3+</sup> ions. The Ti<sup>3+</sup> ions have a long lifetime and bear the photogenerated electrons as a form of energy. The electron transfer process is shown in Equations 6 and 7:



The photovoltage measured as a function of time under visible-light irradiation for FTO/TiO<sub>2</sub>/Cu<sub>2</sub>O and FTO/Cu<sub>2</sub>O electrodes is shown in Figure 5. It can be seen that the potential for both of the two electrodes shifted positively under the same irradiation. The positive potential shift could be due to hole generated on Cu<sub>2</sub>O, which is one of p-type semiconductors. As TiO<sub>2</sub> has no response to visible light, the photopotential of TiO<sub>2</sub>/Cu<sub>2</sub>O bilayer film almost results from Cu<sub>2</sub>O. So, just like Cu<sub>2</sub>O electrode, the potential shift of the TiO<sub>2</sub>/Cu<sub>2</sub>O electrode should be similar to that of Cu<sub>2</sub>O. This result is similar to the report in [32]. The net positive photovoltage results from the interfacial potential difference of electrostatic double layer formed between holes on the surface of Cu<sub>2</sub>O and SO<sub>4</sub><sup>2-</sup> layer in the electrolyte.

**Figure 5.** Photovoltage measured as a function of time for FTO/TiO<sub>2</sub>/Cu<sub>2</sub>O (a) and FTO/Cu<sub>2</sub>O (b) electrodes [36].



Moreover, the potential for the FTO/Cu<sub>2</sub>O electrode jumped to the maximum instantly and remain unchanged. It indicates that the generation and recombination of e<sup>-</sup>-h<sup>+</sup> pairs in Cu<sub>2</sub>O established a dynamic equilibrium. However, it took the FTO/TiO<sub>2</sub>/Cu<sub>2</sub>O electrode about four hours to reach its maximum. It indicates that there was a process for the accumulation of holes in FTO/TiO<sub>2</sub>/Cu<sub>2</sub>O electrode. Since photogenerated electrons and holes were produced in Cu<sub>2</sub>O under the irradiation, it can be proposed that there was a process for the accumulation of electrons in FTO/TiO<sub>2</sub>/Cu<sub>2</sub>O electrode. The photogenerated electrons in Cu<sub>2</sub>O have much energy due to the absorption of visible light. Thus, when these electrons are transferred to the conduct band of TiO<sub>2</sub> and trapped by Ti<sup>4+</sup>, they are seen as Ti<sup>3+</sup> and are stored as a form of energy in the bilayer film. The holes still stay in Cu<sub>2</sub>O. The longer the irradiation time, the more electrons were generated by Cu<sub>2</sub>O and injected into TiO<sub>2</sub> and thereafter the more energy stored. This process did not stop until the potential of the TiO<sub>2</sub>/Cu<sub>2</sub>O electrode reached the maximum.

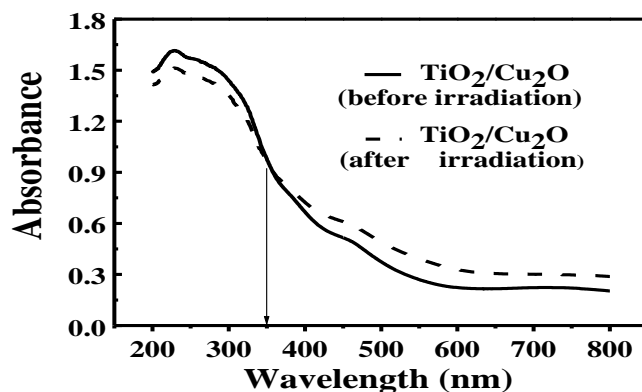
After the irradiation was removed, the potential for both of these electrodes shifted negatively. The potential for FTO/Cu<sub>2</sub>O electrode dropped instantly to the minimum, the original potential before the irradiation. It indicates that the photogenerated electrons and holes are recombined completely. However, it took FTO/TiO<sub>2</sub>/Cu<sub>2</sub>O electrode a long time to reach its minimum, which was still higher than the original potential before the irradiation. It indicates that there are still holes in FTO/TiO<sub>2</sub>/Cu<sub>2</sub>O electrode and the photogenerated electrons and holes may not be recombined completely because a little amount of electrons are still trapped by Ti<sup>3+</sup>.

Additionally, under the same irradiation, the potential increment for FTO/TiO<sub>2</sub>/Cu<sub>2</sub>O electrode was much higher than that for FTO/Cu<sub>2</sub>O electrode. It demonstrates that much more photogenerated holes and electrons were present in the bilayer film. The better photoelectric properties of the bilayer film than that of Cu<sub>2</sub>O film suggests that the bilayer films have improved abilities for charge separation and charge carrier lifetime, and can store energy.

UV-vis diffuse reflectance measurements were further carried out to identify the conversion of Ti<sup>4+</sup> to Ti<sup>3+</sup> in the bilayer film after the irradiation. As shown in Figure 6, the absorbance of the bilayer film became weaker in the short wavelength range (200 nm ≤ λ ≤ 350 nm) while becoming stronger in the long wavelength range (350 nm < λ ≤ 800 nm) after the irradiation. It is confirmed based on the above data that Ti<sup>3+</sup> ions were produced in the bilayer film after the irradiation. Because Ti<sup>4+</sup> has no response to visible light while Ti<sup>3+</sup> does [45-47], the presence of Ti<sup>3+</sup> ions leads to the weaker absorbance of

bilayer film in the short wavelength range while stronger in the long wavelength range. It is found that the transparent TiO<sub>2</sub> film turned blue under the irradiation. The phenomenon is similar to Yasomane'e's report [31] and also demonstrates the presence of Ti<sup>3+</sup>.

**Figure 6.** UV-vis diffuse reflectance spectra of TiO<sub>2</sub>/Cu<sub>2</sub>O bilayer film before (solid line) and after irradiation (dashed line) [36].



As mentioned in the Introduction, similar work was also carried out by Yasomane'e's group. The main phenomena and results are in accord with each other. For example, as for TiO<sub>2</sub>/Cu<sub>2</sub>O composite (or bilayer) film, the color changes under irradiation, the photovoltage curves and hydrogen evolution reactions under irradiation or in dark are similar to each other. However, the explanations for the energy storage between us are different. Yasomane'e proposed that electrons excited by UV-vis light are trapped at electron trapping centres of both Cu<sub>2</sub>O and TiO<sub>2</sub>. These electrons could release under dark and may eventually participate in the hydrogen evaluation reaction in dark. In our work, we demonstrate that Ti<sup>3+</sup> ions in TiO<sub>2</sub>/Cu<sub>2</sub>O bilayer film formed under visible light showed energy storage ability.

#### 4. Energy Storage Property Improvement in TiO<sub>2</sub> Composite System

Since the first bifunctional TiO<sub>2</sub> systems was developed by Xinjing Zou's group, the work on the optimization and improvement of the systems has been carried out. Tatsuma *et al* made a remarkable achievement in this area. For instance, further efforts were taken to optimize the TiO<sub>2</sub>/WO<sub>3</sub> system in order to obtain maximum quantum yield for the electron storage and maximum specific capacity (x in H<sub>x</sub>WO<sub>3</sub>) [29]. To attain the maximum energy storage ability of the TiO<sub>2</sub>/WO<sub>3</sub> system in the gas phase, film composition (W/Ti mole ratio), UV light intensity and film thickness (film mass), were optimized in terms of apparent quantum yield (flux of stored electrons per flux of incident photons), which is an index of the photoelectrochemical charging rate, capacity (maximum charge stored) as well as the specific capacity (x in H<sub>x</sub>WO<sub>3</sub>). According to the experimental results, the maximal apparent quantum yield (~8%) was obtained at a W/Ti ratio = 0.5 and a film thickness ≥10 μm (film mass ≥24 mg cm<sup>-2</sup>). Although a lower light intensity results in a better apparent quantum yield, it leads to slower charging. The capacity was highest at W/Ti = 0.5 and increased with the film thickness. The specific capacity (~0.10) was almost independent of the parameters in the range examined. Considering all these results, it can be concluded that the optimum W/Ti ratio is 0.5 and the film should be thick. In the case where

the electric conductivity of the film is important (e.g., photoelectrochemical protection of metals, in which electrons should be transferred from  $\text{WO}_3$  to the metals), the optimum thickness should be around  $10 \mu\text{m}$  (film mass  $\geq 24 \text{ mg cm}^{-2}$ ).

To improve the applicabilities of the energy storage materials furthermore,  $\text{MoO}_3$ , another energy storage materials that have different discharging potentials, capacities and charging–discharging was rated from those of  $\text{WO}_3$  [23].

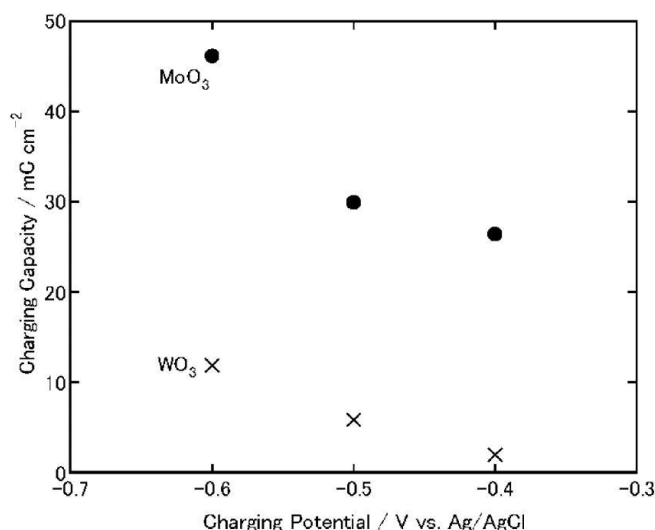
It is known that  $\text{MoO}_3$  and  $\text{WO}_3$  undergo the following redox reactions:



where  $\text{M} = \text{H}, \text{Li}, \text{Na}, \text{etc.}$

As a comparison,  $\text{MoO}_3$  and  $\text{WO}_3$  films were electrochemically charged at  $-0.4$ ,  $-0.5$  or  $-0.6 \text{ V}$  versus  $\text{Ag}|\text{AgCl}$  for 1 h, and discharged at  $1 \mu\text{A}$  (cut-off potential =  $-0.1 \text{ V}$ ; Figures 7 and 8). As the charging potential was shifted more negatively, both the charging and discharging capacities of  $\text{WO}_3$  increased.

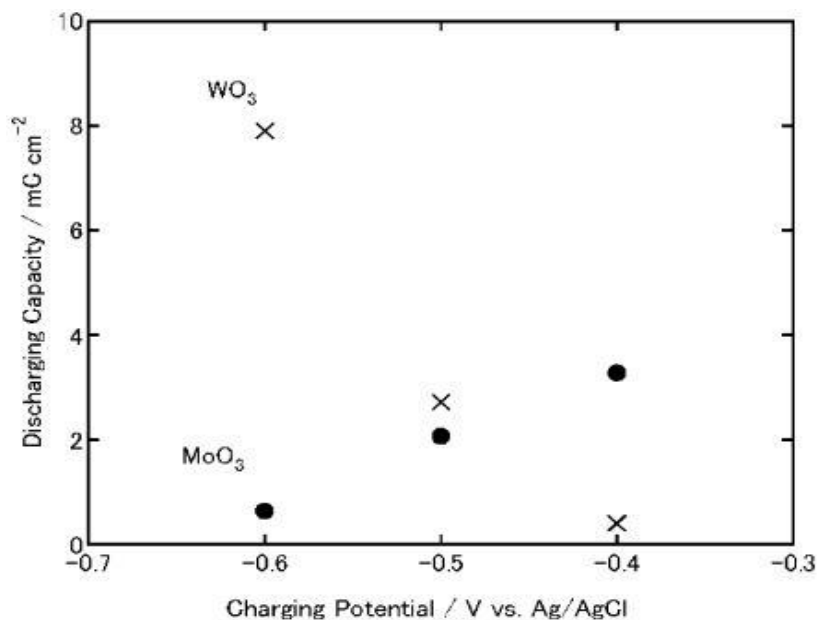
**Figure 7.** Charging capacities of  $\text{MoO}_3$  and  $\text{WO}_3$  coatings on ITO electrodes when the coatings are charged electrochemically (1 h) in 3 wt. %  $\text{NaCl}$  aqueous solutions (pH 5) [23]. Reproduced with permission from Elsevier, © 2004.



On the other hand, in the case of  $\text{MoO}_3$ , its discharging capacity decreased while its charging capacity increased. The discharging efficiency (discharging capacity/charging capacity) of  $\text{WO}_3$  increased constantly as the charging potential was shifted negatively (0.23, 0.46 and 0.66 at  $-0.4$ ,  $-0.5$  and  $-0.6 \text{ V}$ , respectively). However, that of  $\text{MoO}_3$  decreased (0.12, 0.076 and 0.014 at  $-0.4$ ,  $-0.5$  and  $-0.6 \text{ V}$ , respectively). After the discharging, the color of the  $\text{WO}_3$  was almost the same as that before charging while that of the  $\text{MoO}_3$  film was slightly blue, indicating that the film was still partially reduced. Thus, the low discharging efficiency of  $\text{MoO}_3$  may be explained in terms of slow reoxidation or high electrical resistance of  $\text{M}_x\text{MoO}_3$ . In addition, at more negative potentials,  $\text{MoO}_3$  might be partially

reduced to irreversibly intercalated state or to metallic state, which cannot be reoxidized easily to the initial state. Moreover, the fast reoxidation of  $\text{MoO}_3$  by dissolved oxygen during the electrochemical charging may be responsible for the low efficiency.

**Figure 8.** Discharging capacities of  $\text{MoO}_3$  and  $\text{WO}_3$  coatings on ITO electrodes. The coatings were discharged electrochemically at  $1\ \mu\text{A}$  (cut-off potential =  $-0.1\text{V}$  vs.  $\text{Ag}/\text{AgCl}$ ) after electrochemical charging (Figure 3) in 3 wt. %  $\text{NaCl}$  aqueous solution (pH 5) [23]. Reproduced with permission from Elsevier, © 2004.



In either event, when the charging potential is  $-0.4\text{ V}$ , which is the photopotential of  $\text{TiO}_2$ , the charging and discharging capacities of  $\text{MoO}_3$  are one order of magnitude larger than those of  $\text{WO}_3$ . Therefore,  $\text{MoO}_3$  could be used as an energy storage material coupled with  $\text{TiO}_2$ .

For a comparison,  $\text{TiO}_2/\text{MoO}_3$  and  $\text{TiO}_2/\text{WO}_3$  bilayer films were irradiated with UV light for 8 h in air at relative humidity of 80%, and then its open-circuit potential was monitored in a 3 wt. %  $\text{NaCl}$  aqueous solution, respectively. As a result, the self-discharging time of  $\text{TiO}_2/\text{MoO}_3$  bilayer film was elongated to  $>1.5\text{ h}$  (Figure 8). However, the  $\text{TiO}_2/\text{WO}_3$  bilayer film charged under the same conditions exhibited longer self-discharging time than  $\text{TiO}_2/\text{MoO}_3$  film. Thus,  $\text{TiO}_2/\text{MoO}_3$  composite film should be more suitable to be used as energy storage materials in air under humid conditions if the  $\text{MoO}_3$  overlayer is sufficiently thin and the film retains enough adsorbed water on the surface.

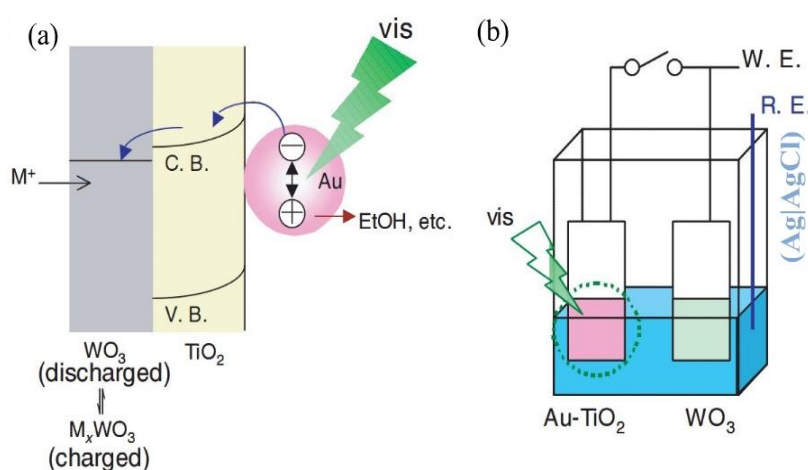
Although  $\text{WO}_3$  has a longer self-discharging time than  $\text{MoO}_3$ ,  $\text{MoO}_3$  exhibited larger charging and discharging capacities and greater ability for oxygen reduction than  $\text{WO}_3$ .  $\text{TiO}_2/\text{MoO}_3$  composite film can also be charged photoelectrochemically in an electrolyte or humid air. Therefore,  $\text{TiO}_2/\text{MoO}_3$  composites may function as energy storage materials under humid conditions.

However,  $\text{TiO}_2$  photocatalyst has some limitations, which come from its own electronic structure. It can work only under UV illumination (wavelength  $< 380\text{ nm}$ ). To overcome the limitation, visible-light responsive  $\text{Au}-\text{TiO}_2$  photocatalyst have been developed [35].

Figure 9a shows the model for visible-light responsive materials with reductive energy storage abilities. The photopotential of the  $\text{TiO}_2$ -coated electrode without Au nanoparticles was  $\sim 0.0\text{ V}$  under

visible light. The open-circuit potential of the Au-TiO<sub>2</sub>-coated electrode was  $\sim +0.1$  V vs. Ag|AgCl in the electrolyte, and the potential shifted to  $\sim -0.2$  V under visible light ( $> 480$  nm;  $\sim 600$  mW cm<sup>-2</sup>). When the Au-TiO<sub>2</sub> film is irradiated, some of the Au nanoparticles are excited by localized surface plasmon resonance (LSPR) and electrons are transferred to TiO<sub>2</sub>. When there is an energy storage material (WO<sub>3</sub>, MoO<sub>3</sub>, and PWA) combined with the Au-TiO<sub>2</sub> film, the reductive energy will be stored. On the other hand, the positive charges left on the Au nanoparticles are consumed by the oxidation of ethanol in the electrolyte, probably to acetic acid.

**Figure 9.** (a) A model for visible-light responsive materials with reductive energy storage abilities. (b) Experimental setup for reductive energy storage in a WO<sub>3</sub> film by a visible-light irradiated Au-TiO<sub>2</sub> film [35]. Reproduced with permission from Elsevier, © 2008.



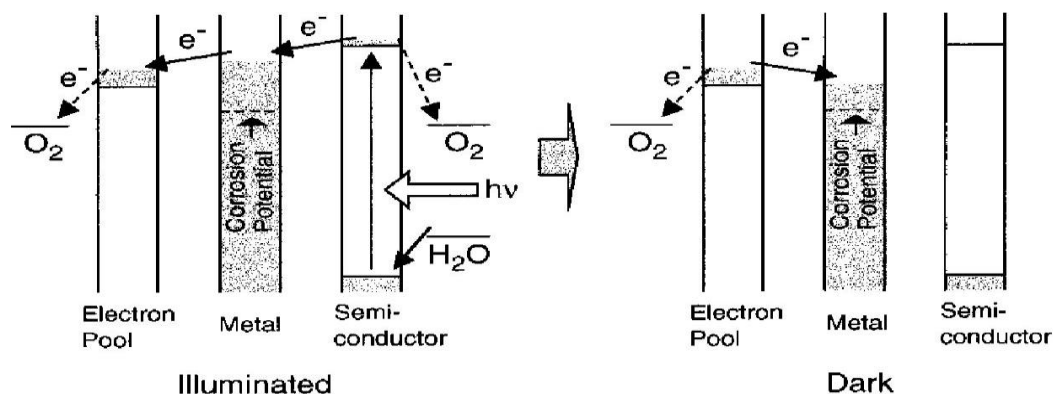
## 5. Application of Energy storage in TiO<sub>2</sub> Composite System

### 5.1. Anticorrosion

Figure 10 illustrates the mechanism of a photoelectrochemical anticorrosion system with energy storage ability. Electrons in the valence band are excited to the conduction band under the irradiation with appropriate light. The excited electrons are injected to the metal so as to keep its potential more negative than the corrosion potential. The excess electrons are accepted by the electron pool (combined WO<sub>3</sub>) so that the reductive energy generated at the irradiated semiconductor can be stored. After the UV light is turned off, electrons stored in WO<sub>3</sub> are injected into the metal so that it is still protected from corrosion. It is obvious that the WO<sub>3</sub> functions in this case as an energy storage device.

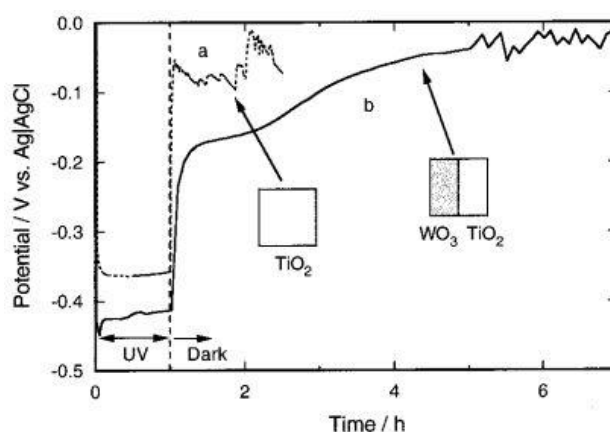
An anticorrosion experiment was carried out using for Type 304 stainless steel as a substrate. Two kinds of samples were prepared. One was coated with TiO<sub>2</sub> and WO<sub>3</sub> (single coating, area, 50% each), and the other was fully coated with TiO<sub>2</sub> (see insets of Figure 11). As Figure 11 shows, the potential of the stainless steel plate fully coated with TiO<sub>2</sub> (curve a) was about 0.4 V vs Ag|AgCl, while the stainless steel is not oxidized during UV irradiation. After the UV light was turned off, however, the potential was shifted in a few minutes to the corrosion potential of the stainless steel.

**Figure 10.** Mechanism of a photoelectrochemical anticorrosion system with an energy storage ability [22].



The potential in the dark was very unstable, indicating that the stainless steel was corroded. In contrast, the potential of the stainless steel plate coated with  $\text{TiO}_2$  and  $\text{WO}_3$  (curve b) was more negative than the corrosion potential for a few hours, even after the light was turned off. Actually, the unstable potential behavior reflecting the corrosion of the substrate stainless steel was not observed for 4 h in dark. These results clearly indicate that the anticorrosion effect of the  $\text{TiO}_2/\text{WO}_3$  system is retained after dark. Potential behavior of the ITO electrode coated with  $\text{TiO}_2$  and  $\text{WO}_3$  (single coating) (area, 50% each) was also examined for comparison. Even though the sample was prepared and tested in the same way as that for the coatings on the stainless steel, it took longer time to be discharged (>6 h). This difference is probably due to a difference in discharging processes. That is, a reduced  $\text{WO}_3$  coating on an ITO electrode is oxidized primarily by oxygen directly while that on a stainless steel plate should be oxidized also by oxygen through the stainless steel. This may be reasonable because stainless steel should catalyze the oxygen reduction more efficiently than ITO.

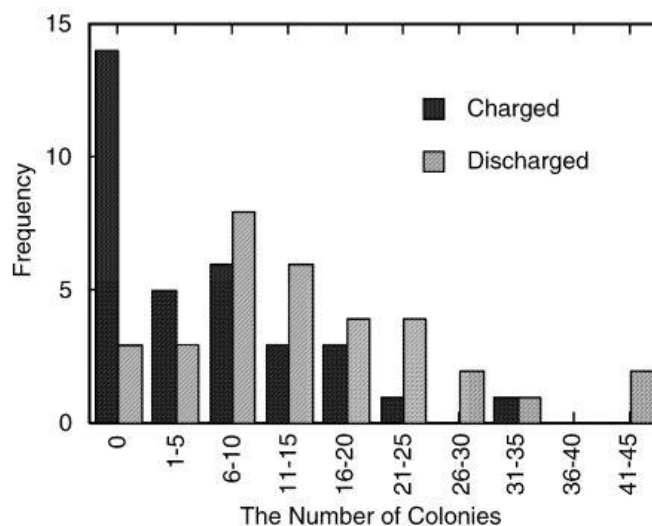
**Figure 11.** Changes in the potential of a type 304 stainless steel ( $1.75 \text{ cm}^2$ ) coated with  $\text{TiO}_2$  (a) and that coated with  $\text{TiO}_2$  and  $\text{WO}_3$  (single coating) (area, 50% each) (b) in an air-saturated 3 wt % NaCl solution, pH 5.  $\text{TiO}_2$  was irradiated with UV light for the first 1 h [22]. Reproduced with permission from the ACS, © 2001.



## 5.2. Bactericidal Effect

Bactericidal effects of the photoelectrochemically charged and discharged  $\text{TiO}_2/\text{WO}_3$  films were examined [28]. A 20  $\mu\text{L}$  aliquot of an *E. coli* suspension was applied onto the film surface, and left for 6 h. The suspension was then transferred onto an agar culture medium and incubated. The number of colonies formed was summarized in the histogram (Figure 12). It is obvious that the survival ratio for the charged sample was lower than that for the discharged sample. The average number of colonies for the control experiment, in which the *E. coli* suspension was directly transferred to the agar culture medium, was 72. Thus, the average survival ratio for the charged samples is 25% while that for the discharged samples is 58%. Although the bactericidal effect is not very strong, multiplication of *E. coli* is suppressed at least in part by the charged  $\text{TiO}_2/\text{WO}_3$  film. The moderate bactericidal effect may prevent bacteria from increasing during the night, and the survived bacteria may be killed by  $\text{TiO}_2$  due to its strong bactericidal effect in the next day.

**Figure 12.** Bactericidal effect of the photoelectrochemically charged (irradiated with UV light for 24 h) and pre-discharged  $\text{TiO}_2/\text{WO}_3$  films. A 20  $\mu\text{L}$  aliquot of *E. coli* suspension that contains  $\sim 70$  cells was applied onto a film surface, and left for 6 h at room temperature, 100% relative humidity. The suspension was then transferred onto a deoxycholate agar culture medium and incubated for 24 h at 37  $^\circ\text{C}$ . The number of thus formed colonies was counted [28]. Reproduced with permission from Elsevier, © 2003.



The bactericidal effect should be based on the reductive energy stored in  $\text{WO}_3$ . Possible reactions proceeding during the discharge of the charged  $\text{WO}_3$  are as follows:



Incidentally, the equimolar amount of protons and electrons are supplied from the reduced  $\text{WO}_3$ ,  $\text{H}_x\text{WO}_3$  (Equation 13):



Among the possible products,  $\text{HO}_2 \cdot$  and  $\text{H}_2\text{O}_2$  have bactericidal effects. Although the consumption of  $\text{O}_2$  could also be responsible for the bactericidal effect, the supply of  $\text{O}_2$  from ambient air should be much faster than the  $\text{O}_2$  consumption. Furthermore,  $\text{HO}_2 \cdot$  and corresponding deprotonated anion  $\text{O}_2^- \cdot$  are less stable than  $\text{H}_2\text{O}_2$ . Therefore,  $\text{H}_2\text{O}_2$  generation from the charged  $\text{TiO}_2/\text{WO}_3$  film was examined.

It is found that in the case of the charged film, the  $\text{H}_2\text{O}_2$  concentration was  $2 \times 10^{-5}$  M while  $\text{H}_2\text{O}_2$  was not detected for the pre-discharged film. Furthermore, the toxicity of  $\text{H}_2\text{O}_2$  for *E. coli* was examined as well. The survival ratios of *E. coli* exposed to various concentrations of  $\text{H}_2\text{O}_2$  for 6 h are summarized in Table 1. Because the average  $\text{H}_2\text{O}_2$  concentration in water on the charged  $\text{TiO}_2/\text{WO}_3$  film during the 6 h treatment may be as low as  $1 \times 10^{-5}$  M, the bactericidal effect of the same film in the dark can be explained mainly in terms of  $\text{H}_2\text{O}_2$  generation.

**Table 1.** Bactericidal effect of  $\text{H}_2\text{O}_2$  solutions of various concentrations <sup>a</sup> [28] Reproduced with permission from Elsevier, © 2003.

$\text{H}_2\text{O}_2$ concentration (M)	Survival ratio <sup>a</sup> (%)
0	65
$1 \times 10^{-6}$	65
$1 \times 10^{-5}$	29
$1 \times 10^{-4}$	3
$1 \times 10^{-3}$	0

<sup>a</sup> *E. coli* was exposed to  $\text{H}_2\text{O}_2$  solutions for 6 h.

### 5.3. Photochromism

When  $\text{TiO}_2$  composite systems were charged under the irradiation and discharged in the dark, the energy storage materials were involved in photoelectrochemical reaction and color changes correspondingly. In addition to the Tatsuma group's reports [27], the photochromic effects of  $\text{TiO}_2/\text{WO}_3$  composite systems were also described in [48,49].

$\text{Ni}(\text{OH})_2$  is known to be an anodic electrochromic material that changes color from colorless to brown upon oxidation [50,51]. The  $\text{Ni}(\text{OH})_2/\text{TiO}_2$  bilayer film was irradiated with UV light (365 nm; 10  $\text{mW cm}^{-2}$ ) [26]. The film turned from colorless (Figure 13a) to brown (Figure 13b) while the electrochemically oxidized film did. However, a  $\text{Ni}(\text{OH})_2$  film without  $\text{TiO}_2$  was electrochemically bleached rapidly and completely. As for the  $\text{Ni}(\text{OH})_2/\text{TiO}_2$  bilayer film, the bleaching was not completed but it was confirmed that the photooxidative coloration and electrochemical bleaching could be repeated at least 5 times. It appears that the  $\text{TiO}_2/\text{Ni}(\text{OH})_2$  bilayer film can potentially be used as a photochromic material.

**Figure 13.**  $\text{TiO}_2/\text{Ni}(\text{OH})_2$  film before (a) and after (b) UV irradiation for 2 h in  $\text{NaHCO}_3/\text{NaOH}$  buffer (pH 10) [26]. Reproduced with permission from the ACS, ©2005.

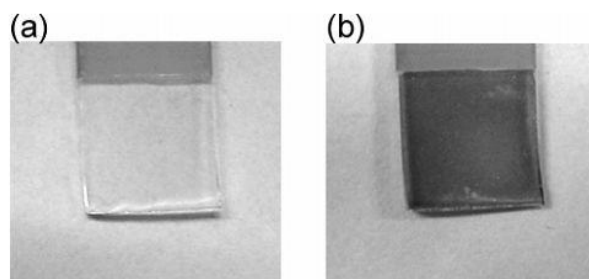


**Figure 14.** Color changes of  $\text{TiO}_2/\text{Ni}(\text{OH})_2$  electrode (a) before irradiation, (b) after irradiation for 1 h and (c) after irradiation for 2 h [33]. Reproduced with permission from Elsevier, © 2009.

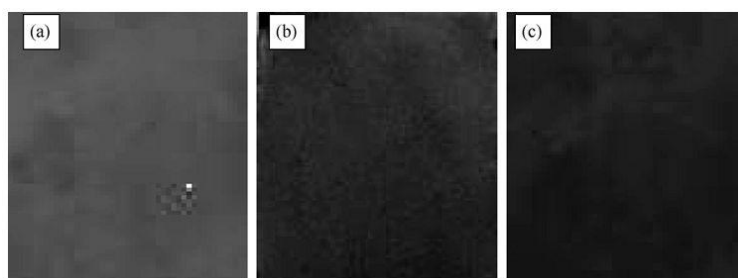


Figure 14 [33] shows the similar color changes of the  $\text{TiO}_2/\text{Ni}(\text{OH})_2$  electrode upon irradiation. Before the irradiation, the color was gray. After 1 h irradiation, it changed to brown. As the irradiation went on for longer times, it eventually changed to dark brown. The gray sample changed to dark brown because of the oxidization of  $\text{Ni}(\text{OH})_2$  to  $\text{NiOOH}$ . The UV-vis absorbance increased as the electrode color becomes darker. The darkening degree of the electrode depended on the light intensity and exposure time. The larger the light intensity or the longer the exposure time, the darker it became.

**Figure 15.** Photograph of three electrode system in photoelectrochemical experiment with persistent visible irradiation for 6 h with (a) low magnification and (b) high magnification [36].

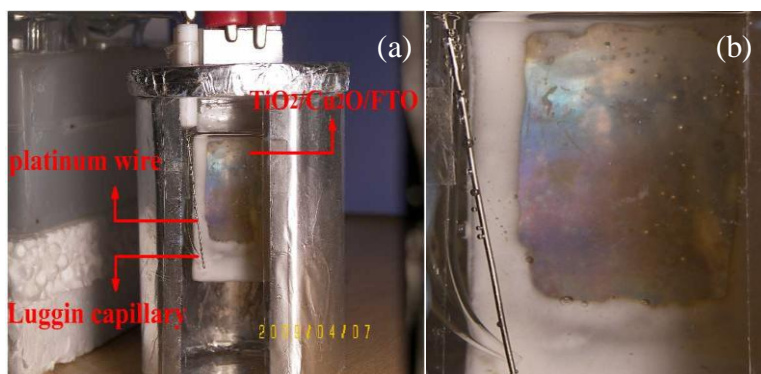
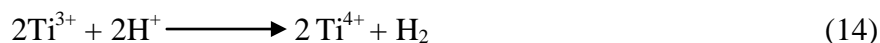
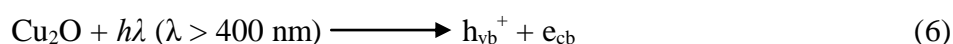


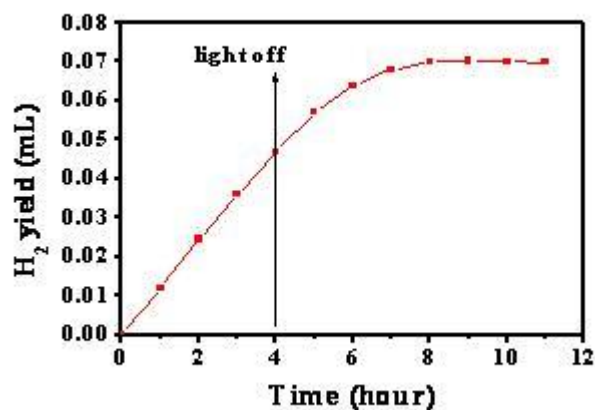
Figure 15 shows a photograph of TiO<sub>2</sub>/Cu<sub>2</sub>O bilayer film [36] in a photoelectrochemical experiment with visible-light irradiation for 6 h. It is found that the transparent TiO<sub>2</sub> film turned blue under the irradiation. The phenomenon is similar to Yasomanee's report [31]. The change of color demonstrates that Ti<sup>4+</sup> in TiO<sub>2</sub> was reduced to Ti<sup>3+</sup> [52,53].

#### 5.4. Photocatalytic H<sub>2</sub> Evolution

As for the application of the energy stored in Ti<sup>3+</sup>, TiO<sub>2</sub>/Cu<sub>2</sub>O bilayer film was used to reduce H<sup>+</sup> for the formation of H<sub>2</sub> from water splitting. The TiO<sub>2</sub>/Cu<sub>2</sub>O bilayer film was immersed in aqueous Na<sub>2</sub>S and Na<sub>2</sub>SO<sub>3</sub> solution and irradiated with visible light. Figure 16 shows the H<sub>2</sub> yield as the function of time under and after the irradiation. It can also be found that H<sub>2</sub> evolution was still noticeable after the irradiation stopped until the third hour. We believe that the electrons trapped in Ti<sup>3+</sup> ions as stored energy leads to H<sub>2</sub> evolution from H<sub>2</sub>O splitting in dark. Based on the mechanism of the energy storage in TiO<sub>2</sub>/Cu<sub>2</sub>O bilayer film proposed in Figure 5, the possible electrons transfer reactions are:



**Figure 16.** Curve of H<sub>2</sub> yield as the function of time under and after visible-light irradiation [36].



The amount of the electrons in Ti<sup>3+</sup> ions as stored energy can be calculated approximately according to the H<sub>2</sub> yield as follows:

$$n = \frac{2 \times V \times N_A}{M \times Q \times S} = \frac{2 \times 0.024 \times 6.02 \times 10^{23}}{22.4 \times 10^3 \times 6.25 \times 10^{18} \times 4} = 5.22 \times 10^{-2}$$

where  $n$  (C cm<sup>-2</sup>) is the amount of electrons/cm<sup>2</sup> trapped in Ti<sup>3+</sup> ions in TiO<sub>2</sub>/Cu<sub>2</sub>O film,  $V$  is the volume of H<sub>2</sub> produced in the dark,  $Q$  is the number of electrons per coulomb,  $S$  is the surface area of TiO<sub>2</sub>/Cu<sub>2</sub>O bilayer film,  $M$  and  $N_A$  are the molar volume of a gas in standard conditions and Avogadro constant respectively. The calculated result indicates that more than  $5 \times 10^{-2}$  C cm<sup>-2</sup> electrons were stored in TiO<sub>2</sub>/Cu<sub>2</sub>O film under 4 h visible-light irradiation.

## 6. Concluding Remarks

The progress made on the energy storage in bifunctional modified TiO<sub>2</sub> systems under UV light and visible light is summarized. Substantially, this research has the advantage of the combination of the dual functions of opto-electric conversion and energy storage together in a single system. Moreover, cheap composite thin films based on TiO<sub>2</sub> and other metal oxide semiconductor may utilize solar energy and take the place of accumulators for energy storage in some special applications. However, it can be seen from the current literatures on this subject is still in its infancy, although it is full of hope. We believe this subject warrants more extended and in-depth study in the future, comparable to the efforts that have been taken on the separate areas of photoelectric conversion and solar energy storage, respectively [54-58].

We may need to continue this study focusing on two aspects. On one hand, the working mechanism of the reported systems has yet not been understood fully and needs further study. In addition, some of these results reviewed here may turn out to be of mere fundamental interest and relevant for the a particular environment, application or problem. Some might be helpful for understanding the properties of the modified TiO<sub>2</sub> energy storage materials [59-62]. On the other hand, a concerted effort is needed to screen potential useful bifunctional systems and find ways to design relevant devices for practical applications, which may begin with material preparation. Also, nanostructured architectures should be considered to be synthesized for the composition of the bifunctional TiO<sub>2</sub> composite material for the improvement of opto-electric conversion and energy storage property.

Anyway, although research has only just begun to explore the science and engineering applications of this remarkable material platform, we do hope this review can promote more fundamental and applied lines of research on this subject in the coming future.

## Acknowledgements

We acknowledge the financial supports from National Natural Science Foundation of China (Grant Nos 20973070 and 90510012), National Basic Research Program of China (No. 2009CB939704), the Key Project of Chinese Ministry of Education (No. 109116) and the Programme of Introducing Talents of Discipline to Universities (No. B08033).

## References

1. Weisz, P.B. Basic choices and constraints on long-term energy supplies. *Phys. Today*. **2004**, *57*, 47-52.
2. Bartlett, A.A. Sustained availability: A management program for nonrenewable resources. *Am. J. Phys.* **1986**, *54*, 398-402.
3. Dresselhaus, M.S.; Thomas, I.L. Alternative energy technologies. *Nature*. **2001**, *414*, 332-337.
4. Lewis, N.S.; Crabtree, G.W.; Nozik, A.J.; Wasielewski, M.R.; Alivisatos, A.P. *Basic Energy Sciences Report on Basic Research Needs for Solar Energy Utilization*; Office of Science, U.S. Department of Energy: Washington, DC, USA, 2005; Available online: [http://www.sc.doe.gov/bes/reports/files/SEU\\_rpt.pdf](http://www.sc.doe.gov/bes/reports/files/SEU_rpt.pdf) (accessed on 19 August 2009).

5. Kamat, P.V. Meeting the clean energy demand: Nanostructure architectures for solar energy conversion. *J. Phys. Chem. C* **2007**, *111*, 2834-2860.
6. Aberle, G.A. Thin-film solar cells. *Thin Solid Films* **2009**, *517*, 4706-4710.
7. Green, M.A.; Zhao, J.; Wang, A.; Wenham, S.R. Progress and outlook for high-efficiency crystalline silicon solar cells. *Sol. Energy Mater. Sol. Cells* **2001**, *65*, 9-16.
8. Nij, J.F.; Szlufcik, J.; Poortmans, J.; Sivothythaman, S.; Mertens, R.P. Advanced cost-effective crystalline silicon solar cell technologies. *Sol. Energy Mater. Sol. Cells* **2001**, *65*, 249-259.
9. Grätzel, M. Solar energy conversion by dye-sensitized photovoltaic cells. *Inorg. Chem.* **2005**, *44*, 6841-6851.
10. Ibrahim, H.; Ilinca, A.; Perron, J. Energy storage systems—Characteristics and comparisons. *Renew. Sustain. Energy Rev.* **2008**, *12*, 1221-1250.
11. Tachikawa, T.; Fujitsuka, M.; Majima, T. Mechanistic insight into the  $\text{TiO}_2$  photocatalytic reactions: Design of new photocatalysts. *J. Phys. Chem. C* **2007**, *111*, 5259-5275.
12. Serpone, N. Is the band gap of pristine  $\text{TiO}_2$  narrowed by anion- and cation-doping of titanium dioxide in second-generation photocatalysts? *J. Phys. Chem. B* **2006**, *110*, 24287-24293.
13. Hirakawa, T.; Kamat, V.P. Charge separation and catalytic activity of  $\text{Ag@TiO}_2$  core-shell composite clusters under uv-irradiation. *J. Am. Chem. Soc.* **2005**, *127*, 3928-3934.
14. Subramanian, V.; Wolf, E.E.; Kamat, V.P. Catalysis with  $\text{TiO}_2$ /Gold nanocomposites. Effect of metal particle size on the fermi level equilibration. *J. Am. Chem. Soc.* **2004**, *126*, 4943-4950.
15. Zhao, W.; Ma, W.; Chen, C.; Zhao, J.; Shuai, Z. Efficient degradation of toxic organic pollutants with  $\text{Ni}_2\text{O}_3/\text{TiO}_{2-x}\text{B}_x$  under visible irradiation. *J. Am. Chem. Soc.* **2004**, *126*, 4782-4783.
16. István, R.; Kuno, M.; Kamat, V.P. Size-dependent electron injection from excited cdse quantum dots into  $\text{TiO}_2$  nanoparticles. *J. Am. Chem. Soc.* **2007**, *129*, 4136-4137.
17. Robel, I.; Subramanian, V.; Kuno, M.; Kamat, V.P. Quantum dot solar cells. Harvesting light energy with CdSe. *J. Am. Chem. Soc.* **2006**, *128*, 2385-2393.
18. Trinchi, A.; Li, Y.X.; Wlodarski, W.; Kaciulis, S.; Pandolfic, L.; Viticoli, S.; Comini, E.; Sberveglieri, G. Investigation of sol-gel prepared  $\text{CeO}_2\text{-TiO}_2$  thin films for oxygen gas sensing. *Sens. Actuat. B* **2003**, *95*, 145-150.
19. Mor, K.G.; Varghese, K.O.; Paulose, M.; Shankar, K.; Grimes, A.C. A review on highly ordered, vertically oriented  $\text{TiO}_2$  nanotube arrays: Fabrication, material properties and solar energy applications. *Sol. Energy Mater. Sol. Cells* **2006**, *90*, 2011-2075.
20. Ni, M.; Leung, M.K.H.; Leung, D.Y.C.; Sumathy, K. A review and recent developments in photocatalytic water-splitting using  $\text{TiO}_2$  for hydrogen production. *Renew. Sustain. Energy Rev.* **2007**, *11*, 401-425.
21. Zou, X.J.; Maesako, N.; Nomiya, T.; Horie, Y.; Miyazaki, T. Photo-rechargeable battery with  $\text{TiO}_2$ /carbon fiber electrodes prepared by laser deposition. *Sol. Energy Mater. Sol. Cells* **2000**, *62*, 133-142.
22. Tatsuma, T.; Saitoh, S.; Ohko, Y.; Fujishima, A.  $\text{TiO}_2\text{-WO}_3$  photoelectrochemical anticorrosion system with an energy storage ability. *Chem. Mater.* **2001**, *13*, 2838-2842.
23. Takahashi, Y.; Ngaotrakanwivat, P.; Tatsuma, T. Energy storage  $\text{TiO}_2\text{-MoO}_3$  photocatalysts. *Electrochim. Acta* **2004**, *49*, 2025-2029.

24. Ohko, Y.; Saitoh, S.; Tatsuma, T.; Fujishima, A. SrTiO<sub>3</sub>-WO<sub>3</sub> photocatalysis systems with an energy storage ability. *Electrochemistry* **2002**, *70*, 460-462.
25. Ngaotrakanwiat, P.; Saitoh, S.; Ohko, Y.; Tatsuma, T.; Fujishim, A. TiO<sub>2</sub>-phosphotungstic acid photocatalysis systems with an energy storage ability. *J. Electrochem. Soc.* **2003**, *150*, A1405-A1407.
26. Takahashi, Y.; Tatsuma, T. Oxidative energy storage ability of a TiO<sub>2</sub>-Ni(OH)<sub>2</sub> bilayer photocatalyst. *Langmuir* **2005**, *21*, 12357-12361.
27. Tatsuma, T.; Saitoh, S.; Ngaotrakanwiat, P.; Ohko, Y.; Fujishima, A. Energy storage of TiO<sub>2</sub>-WO<sub>3</sub> photocatalysis systems in the gas phase. *Langmuir* **2002**, *18*, 7777-7779.
28. Tatsuma, T.; Taked, S.; Saitoh, S.; Ohko, Y.; Fujishima, A. Bactericidal effect of an energy storage TiO<sub>2</sub>-WO<sub>3</sub> photocatalyst in dark. *Electrochem. Commun.* **2003**, *5*, 793-796.
29. Ngaotrakanwiat, P.; Tatsuma, T. Optimization of energy storage TiO<sub>2</sub>-WO<sub>3</sub> photocatalysts and further modification with phosphotungstic acid. *J. Electroanal. Chem.* **2004**, *573*, 263-269.
30. Subasri, R.; Shinohara, T. Investigations on SnO<sub>2</sub>-TiO<sub>2</sub> composite photoelectrodes for corrosion protection. *Electrochem. Commun.* **2003**, *5*, 897-902.
31. Yasomanee, J.P.; Bandara, J. Multi-electron storage of photoenergy using Cu<sub>2</sub>O-TiO<sub>2</sub> thin film photocatalyst. *Sol. Energy Mater. Sol. Cells* **2008**, *92*, 348-352.
32. Wang, C.T.; Huang, H.H. Photo-chargeable titanium/vanadium oxide composites. *J. Non-Cryst. Solid.* **2008**, *354*, 3336-3342.
33. Zhang, W.K.; Wang, L.; Huang, H.; Gan, Y.P.; Wang, C.T.; Tao, X.Y. Light energy storage and photoelectrochemical behavior of the titanate nanotube array/Ni(OH)<sub>2</sub> electrode. *Electrochim. Acta* **2009**, *54*, 4760-4763.
34. Zhao, D.; Chen, C.C.; Yu, C.L.; Ma, W.H.; Zhao, J.C. Photoinduced electron storage in WO<sub>3</sub>/TiO<sub>2</sub> nanohybrid material in the presence of oxygen and postirradiated reduction of heavy metal ions. *J. Phys. Chem. C* **2009**, *113*, 13160-13165.
35. Takahashi, Y.; Tatsuma, T. Visible light-induced photocatalysts with reductive energy storage abilities. *Electrochem. Commun.* **2008**, *10*, 1404-1407.
36. Xiong, L.B.; Ouyang, M.L.; Yan, L.L.; Li, J.L.; Qiu, M.Q.; Yu, Y. Visible-light energy storage by Ti<sup>3+</sup> in TiO<sub>2</sub>/Cu<sub>2</sub>O bilayer film. *Chem. Lett.* **2009**, *38*, 1154-1155.
37. Zhao, C.J.; Gu, Y.; Chen, H.; Jiang, Z.Y. Thermal effects on the measurement of photocurrent at anodic films on nickel electrodes. *Electrochim. Acta* **2002**, *47*, 1801-1809.
38. Carpenter, M.K.; Corrigan, D.A. Photoelectrochemistry of nickel hydroxide thin films. *J. Electrochem. Soc.* **1989**, *136*, 1021-1026.
39. Madou, M.J.; McKubre, M.C.H. Impedance measurements and photoeffects on Ni electrodes. *J. Electrochem. Soc.* **1983**, *130*, 1056-1061.
40. Uekawa, N.; Suzuki, T.; Ozeki, S.; Kaneko, K. Rectification effect by a p-n junctioned oxide film. *Langmuir* **1992**, *8*, 1-3.
41. Jing, L.Q.; Sun, X.J.; Cai, W.M.; Xu, Z.L.; Du, Y.G.; Fu, H.G. The preparation and characterization of nanoparticle TiO<sub>2</sub>/Ti films and their photocatalytic activity. *J. Phys. Chem. Solids.* **2003**, *64*, 615-623.

42. Nair, M.T.S.; Guerrero, L.; Arenas, O.L.; Nair, P.K. Chemically deposited copper oxide thin films: Structural, optical and electrical characteristics. *Appl. Surf. Sci.* **1999**, *150*, 143-151.
43. Grätzel, M. Photoelectrochemical cells. *Nature* **2001**, *414*, 338-344.
44. Zhang, L.S.; Li, J.L.; Chen, Z.G.; Tang, Y.W.; Yu, Y. Preparation of Fenton reagent with H<sub>2</sub>O<sub>2</sub> generated by solar light-illuminated nano-Cu<sub>2</sub>O/MWNTs composites. *Appl. Catal. A. Gen.* **2005**, *299*, 292-297.
45. Kuznetsov, A.I.; Kameneva, O.; Alexandrov, A.; Bityurin, N.; Chhor, K.; Kanaev, A. Chemical activity of photoinduced Ti<sup>3+</sup> centers in titanium oxide gels. *J. Phys. Chem. B.* **2006**, *110*, 435-441.
46. Kuznetsov, A.I.; Kameneva, O.; Rozes, L.; Sanchez, C.; Bityurin, N.; Kanaev, A. Extinction of photo-induced Ti<sup>3+</sup> centres in titanium oxide gels and gel-based oxo-PHEMA hybrids. *Chem. Phys. Lett.* **2006**, *429*, 523-527.
47. Kuznetsov, A.I.; Kameneva, O.; Alexandrov, A.; Bityurin, N.; Marteau, P.; Chhor, K.; Sanchez, C.; Kanaev, A. Light-induced charge separation and storage in titanium oxide gels. *Phys. Rev. E* **2005**, *71*, 0214031-0214037.
48. He, T.; Ma, Y.; Cao, Y.A.; Hu, X.L.; Liu, H.M.; Zhang, G.J.; Yang, W.S.; Yao, A.N. Photochromism of WO<sub>3</sub> colloids combined with TiO<sub>2</sub> nanoparticles. *J. Phys. Chem. B* **2002**, *106*, 12670-12676.
49. Bechinger, C.; Ferrere, S.; Zaban, A.; Sprague, J.; Gregg, B.A. Photoelectrochromic windows and displays. *Nature* **1996**, *383*, 608-610.
50. Porqueras, I.; Bertran, E. Electrochromic behaviour of nickel oxide thin films deposited by thermal evaporation. *Thin Solid Films* **2001**, *398-399*, 41-44.
51. Ragan, D.D.; Svedlindh, P.; Graqvist, C.G. Electrochromic Ni oxide films studied by magnetic measurements. *Sol. Energy Mater. Sol. Cells* **1998**, *54*, 247-254.
52. Bityurin, N.; Kuznetsov, A.I.; Kanaev, A. Kinetics of UV-induced darkening of titanium-oxide gels. *Appl. Surf. Sci.* **2005**, *248*, 86-90.
53. Bityurin, N.; Znaidi, L.; Kanaev, A. Laser-induced absorption in titanium oxide based gels. *Chem. Phys. Lett.* **2003**, *374*, 95-99.
54. Richard, E.; Nocera, D.G. Preface: Overview of the forum on solar and renewable energy. *Inorg. Chem.* **2005**, *44*, 6799-6801.
55. Kazempour, S.J.; Moghaddam, M.P.; Haghifam, M.R.; Yousefi, G.R. Electric energy storage systems in a market-based economy: Comparison of emerging and traditional technologies. *Renew. Energ.* **2009**, *34*, 2630-2639.
56. Granqvist, C.G.; Wittwer, V. Materials for solar energy conversion: An overview. *Sol. Energy Mater. Sol. Cells* **1998**, *54*, 39-48.
57. Baker, J. New technology and possible advances in energy storage. *Energ. Policy* **2008**, *36*, 4368-4373.
58. Hadjipaschalis, I.; Poullikkas, A.; Efthimiou, V. Overview of current and future energy storage technologies for electric power applications. *Renew. Sustain. Energ. Rev.* **2009**, *13*, 1513-1522.
59. Miyasaka, T.; Murakami, T.N. The photocapacitor: An efficient self-charging capacitor for direct storage of solar energy. *Appl. Phys. Lett.* **2004**, *85*, 3932-3934.

60. Dhanabalan, A.; Dos Santos, D.S.; Mendonca, C.R., Jr.; Misoguti, L.; Balogh, D.T.; Giacometti, J.A.; Zilio, S.C.; Oliveira, O.N., Jr. Optical storage in mixed Langmuir-Blodgett (LB) films of disperse Red-19 isophorone polyurethane and cadmium stearate. *Langmuir* **1999**, *15*, 4560-4564.
61. Xie, Y.B.; Huang, C.J.; Zhou, L.M.; Liu, Y.; Huang, H.T. Supercapacitor application of nickel oxide–titania nanocomposites. *Compos. Sci. Technol.* **2009**, *69*, 2108-2114.
62. Hirakawa, T.; Kamat, P.V. Photoinduced electron storage and surface plasmon modulation in Ag@TiO<sub>2</sub> Clusters. *Langmuir* **2004**, *20*, 5645-5647.

© 2009 by the authors; licensee Molecular Diversity Preservation International, Basel, Switzerland. This article is an open-access article distributed under the terms and conditions of the Creative Commons Attribution license (<http://creativecommons.org/licenses/by/3.0/>).